Scaling Laws for Unstable Interfaces Driven by Strong Shocks in Cylindrical Geometry

Qiang Zhang[1] and Mary Jane Graham[2,3]
[1]*Department of Applied Mathematics and Statistics, State University of New York at Stony Brook, Stony Brook, New York 11794-3600*
[2]*Department of Mathematical Sciences, United States Military Academy, West Point, New York 10996-1786*
[3]*Army Research Laboratory, Aberdeen Proving Ground, Maryland 21005-5066*
(Received 21 March 1997; revised manuscript received 14 July 1997)

The Richtmyer-Meshkov (RM) instability is an interfacial interface between two fluids of different densities driven by shock waves and plays an important role in the studies of inertial confinement fusion and of supernovas. So far, most of the studies are for RM unstable interfaces driven by weak or intermediate shocks in planar geometry. For experiments conducted at the Nova laser, the unstable material interface is accelerated by very strong shocks. In this Letter, we present scaling laws for the RM unstable interface driven by strong imploding and exploding shocks. [S0031-9007(97)04092-1]

PACS numbers: 47.40.Nm, 47.11.+j, 47.20.Ma

The study of Richtmyer-Meshkov (RM) instabilities has attracted many researchers in recent years, due to the fact that this instability plays an important role in inertial confinement fusion and supernovas. Experimental studies of the RM unstable interface driven by strong shocks (Mach number > 20) have been achieved [1]. With the rapid advances in computing technology, direct numerical simulation has become popular. It provides us with a new way to study RM unstable systems. Most of the numerical studies of the RM unstable system have been and are being performed in planar geometry and for incident shocks with small or intermediate Mach number. In this Letter, we consider the RM unstable interface driven by strong shocks in cylindrical geometry and establish an important scaling law. This scaling law will allow researchers to significantly reduce the number of experiments and numerical simulations required in the study of RM unstable interfaces driven by strong shocks.

The instability of a material interface under an acceleration of an incident shock was predicted theoretically by Richtmyer [2] and confirmed experimentally by Meshkov [3]. Several theories have been developed by different approaches [4–12]; various experiments have been designed to study the RM instability [3,13–16], and numerical simulations have been conducted [5,17–22].

The method of front tracking [23] has been used in our numerical simulations. Front tracking is an adaptive computational method where a low dimensional, moving grid is embedded in a high dimensional fixed grid. The low dimensional, moving grid is fitted to and moves dynamically with the discontinuity fronts in the flow—such as the material interface, where the density is discontinuous, or the shock interface, where the pressure is discontinuous. In these studies, a front can also be the leading or trailing edges of a rarefaction wave. The front tracking method uses the exact mathematical property, known as the Riemann problem solution, to advance the position of the discontinuity interface and to update the physical quantities on each side of the interface. See [23] for further details of the front tracking method and its implementation.

The presence of geometric curvature complicates the systems considerably. There are four different classes of RM unstable systems in a curved geometry: class 1, a shock wave exploding from a light fluid to a heavy fluid; class 2, a shock wave imploding from a light fluid to a heavy fluid; class 3, a shock wave exploding from a heavy fluid to a light fluid; and class 4, a shock wave imploding from a heavy fluid to a light fluid. The classification given here is also applicable to the RM instability in spherical geometry. Because of the symmetry along the x and y axes, Neumann boundary conditions are chosen at $x = 0$ and $y = 0$, allowing the solution to be computed in the first quadrant. Note that in planar geometry, there are two classes of RM unstable systems: A shock wave collides with the material interface from the light fluid phase to the heavy fluid phase, and a shock wave collides with the material interface from the heavy phase fluid to the light phase fluid.

The general features of the development of the RM interface in cylindrical geometry are the following. As an incident shock collides with the material interface, it bifurcates into a transmitted shock and a reflected wave. This stage is known as a wave bifurcation stage, or a shock-contact interaction stage. Depending on the material properties of the fluids across the material interface and the incident shock strength, the reflected shock can be either a shock or a rarefaction wave. For the majority of real gases, the criterion is that when the shock collides with the material interface from the light fluid phase to the heavy fluid phase, the reflected wave is a shock; otherwise, it is a rarefaction wave. Here heavy and light are measured in terms of acoustic impedance, ρc, where ρ is the density of a fluid, and c is the speed of sound. Therefore, in classes 1 and 2 both the transmitted wave and the reflected wave are shocks. In classes 3 and

 0031-9007/97/79(14)/2674(4)$10.00

4 the transmitted wave is a shock while the reflected wave is rarefaction wave. A general theory on the reflected wave type can be found in Ref. [6].

At the end of the bifurcation stage, both the transmitted shock and the reflected wave detach from the material interface. One wave propagates toward the origin, and the other wave propagates away from the origin. For an open space, this outgoing wave will not interact with the material interface again. Accelerated by the incident shock, the material interface becomes unstable and fingers grow to form bubbles of light fluid and spikes of heavy fluid. The wave which moves toward the origin bounces back from the origin. As the bounced wave propagates outward, it interacts with the material interface again, which is known as reshock. Wave bifurcation occurs again, and so on. Therefore, the occurrence of reshock is unavoidable in curved geometry.

How will the incident shock strength affect the development of RM instability? In general, the stronger the incident shock is, the faster the material interface will be accelerated, and the faster the transmitted shock and reflected rarefaction wave travel. The phenomena of reshock will occur at earlier time for systems accelerated by strong shocks. Therefore, dimensional units are not appropriate for studying the scaling behavior of an RM unstable system driven by the strong shocks. In order to reveal the scaling behavior of RM unstable systems, we introduce the following scaled dimensionless quantities:

$$\tilde{r} = r/R_0\,, \qquad \tilde{v} = v/W_i\,, \qquad \tilde{t} = W_i t/R_0\,.$$

Here R_0 is the mean radius of the initial material interface at $t = 0$, and W_i is the speed of the incident shock. In these scaled dimensionless units, the initial location of the material interface is given by $\tilde{r} = 1 + \tilde{a}_0 \cos(m\phi)$. Here $\tilde{a}_0 = a_0/R_0$ is a dimensionless perturbation amplitude, and a_0 is a dimensional perturbation amplitude.

The size of the mixing zone between the light and heavy fluids, i.e., the radial distance of the peaks and valleys along the material interface is a very important quantity for the RM unstable system. We define the overall growth rate and the amplitude of the RM unstable interface in cylindrical geometry as

$$v = (\dot{r}_{\max} - \dot{r}_{\min})/2 \quad \text{and} \quad a = (r_{\max} - r_{\min})/2\,,$$

respectively. Then the scaled dimensionless overall growth rate and amplitude are given by

$$v = (\dot{r}_{\max} - \dot{r}_{\min})/2W_i \quad \text{and} \quad a = (r_{\max} - r_{\min})/2R_0\,,$$

respectively.

Figure 1 shows the perturbation growth rate for all four classes. For all simulations the light fluid is air and the heavy fluid is SF_6. The results for the growth rate of the RM interface driven by an incident shock of Mach number $M = 1.2$, 10, 15, 40, and 100 are superimposed in Fig. 1 and are shown in terms of scaled velocity and

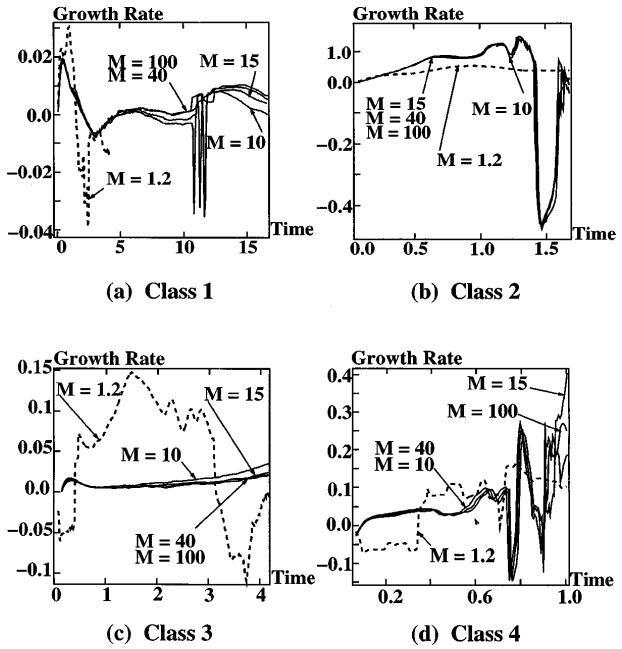

FIG. 1. Comparison of the scaled perturbation growth rate versus scaled time for various Mach numbers—namely, $M = 1.2$, 10, 15, 40, and 100. The dashed curves are for $M = 1.2$. The preshocked Atwood number of the air-SF_6 interface is $A = 0.672\,13$.

scaled time. The numerical simulations are conducted at a dimensionless grid spacing $\Delta\tilde{x} = \Delta\tilde{y} = \Delta x/R_0 = 0.0042$. At this resolution, the numerical solution is no longer sensitive to the grid size. The initial (preshocked) dimensionless perturbation amplitude is $a/R_0 = 0.033$. In Fig. 2 we show the corresponding scaled dimensionless

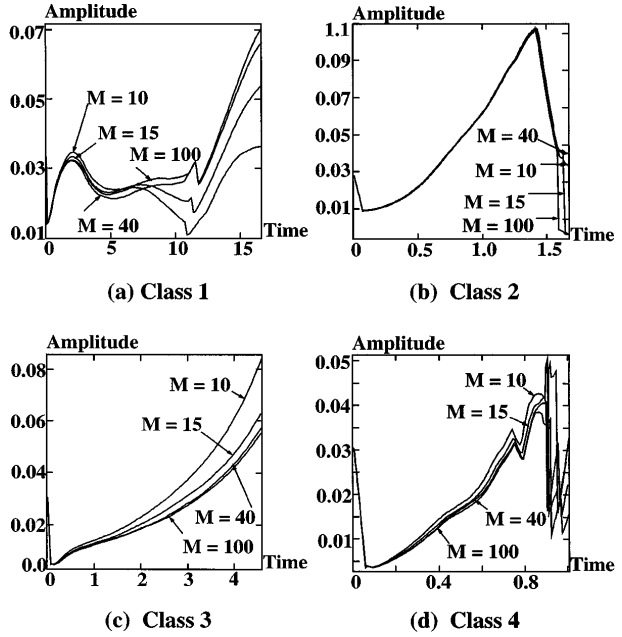

FIG. 2. Comparison of the perturbation amplitude versus time for various Mach numbers—namely, $M = 10$, 15, 40, and 100.

perturbation amplitude as a function of the scaled time. Figures 1 and 2 showed that in the imploding (exploding) case, once the Mach number of the incident shock is larger than 15 (40), the scaled quantities are no longer sensitive to the incident shock strength. Therefore, RM unstable systems driven by strong shocks satisfy a nice scaling law. Let $v_{M_1}(t)$ be the growth rate of a RM unstable interface driven by a strong shock of Mach number M_1, where both v and t are dimensional quantities. Then the overall growth rate, $v_{M_2}(t)$, for a RM unstable interface driven by a strong shock of Mach number M_2 can be obtained from $v_{M_1}(t)$ by the scaling relation,

$$v_{M_2}(t) = \frac{M_1}{M_2} v_{M_1}\left(\frac{M_1}{M_2} t\right). \tag{1}$$

Similarly, the following scaling relation holds for the amplitudes:

$$a_{M_2}(t) = a_{M_1}\left(\frac{M_1}{M_2} t\right). \tag{2}$$

The results shown in Figs. 2 and 3 are for the overall growth rate and amplitude of the RM unstable interface, which are global features. Will the shape of the interface also satisfy a scaling law? Our numerical simulations showed that it indeed does. In Fig. 3, we superimpose the shapes of the class 2 RM unstable interfaces driven by strong shocks of Mach number, $M = 10$, 15, 40, and 100. The inner and outer curves in Fig. 3 are transmitted and reflected shock waves, respectively, and the curves between them are the material interfaces. The snapshots of the interfaces at four different times $\tilde{t} = 0.57$, 0.83, 1.0, and 1.3 are shown in Fig. 3. It is obvious from Fig. 3 that the following scaling law holds for the shape of the unstable interface:

$$\vec{R}_{M_2} = \vec{R}_{M_1}\left(\frac{M_1}{M_2} t\right). \tag{3}$$

Here $\vec{R}$ represents the location for the material interface, the shock waves, or rarefaction wave. For comparison, the shape of the unstable material interface driven by a weak shock of Mach number 1.2 is shown in Fig. 4 at the same scaled times. By comparing Fig. 3 with Fig. 4, we conclude that the shape of RM unstable interface driven by strong shocks and that driven by weak shocks are quite different. Therefore, the scaling law presented above does not hold for RM unstable interfaces driven by weak shocks.

The critical Mach number above which the scaling laws hold is a function of Atwood number, adiabatic exponents of the two fluids, and geometry. The preshocked Atwood

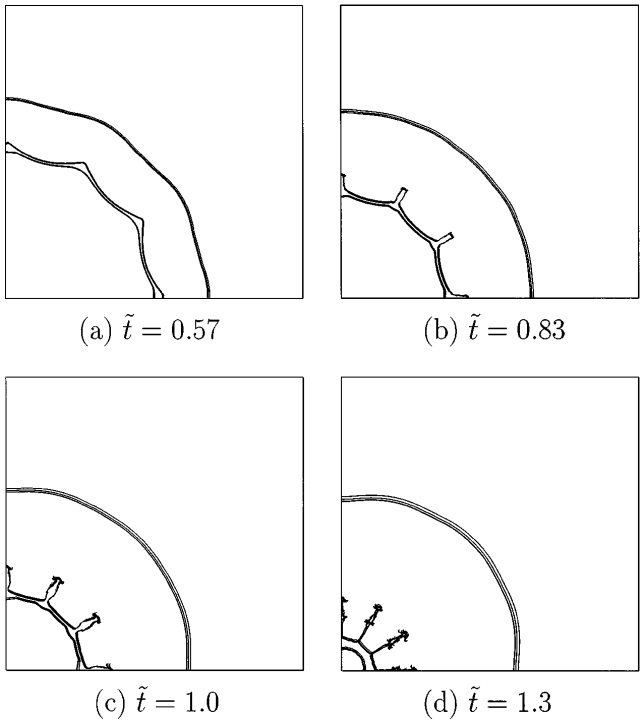

FIG. 3. Evolution of the interfaces for class 2 (light-imploding-heavy), where Mach numbers 10, 15, 40, and 100 are superimposed at various dimensionless times. The incident shock has bifurcated into a transmitted shock moving radially toward the origin and a reflected shock moving radially away from the origin. In terms of scaled time, the interfaces driven by different Mach number ($M \geq 10$) coincide and demonstrate a scaling law.

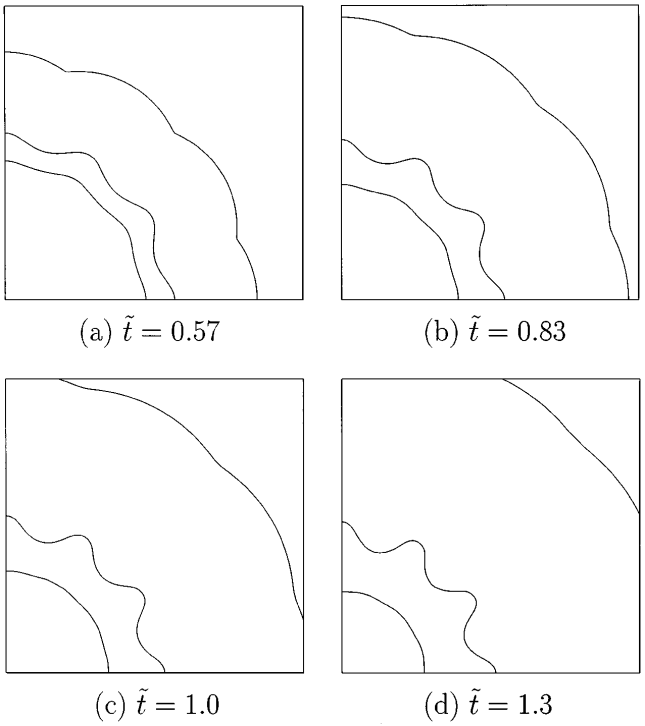

FIG. 4. Evolution of the interface for class 2 (light-imploding-heavy) for Mach number 1.2. The frames shown in this figure are at the same dimensionless time as in Fig. 3. Note that the shape of the interface is quite different from those in Fig. 3. Therefore, the scaling law does not hold for weak shocks.

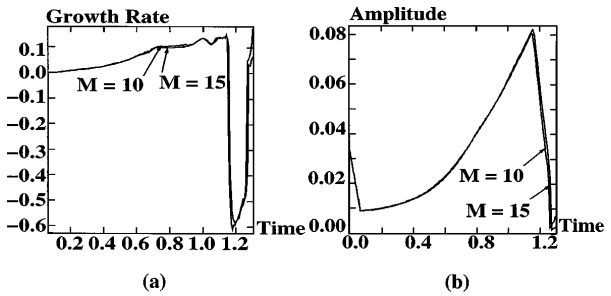

FIG. 5. Comparison of the scaled growth rate and the scaled perturbation growth rate versus scaled time for Mach numbers $M = 10$ and 15. Here the preshocked Atwood number is $A = 0.333\,33$.

number between air-SF_6 is $A = 0.672\,13$. To further confirm the scaling laws given by (1)–(3), we present the results for the system in class 2 with preshocked Atwood number $A = 0.333\,33$ in Fig. 5. The adiabatic exponents of the two fluids are the same as those of air and SF_6. Figure 5 shows that the scaling laws are indeed satisfied once the Mach number is larger than 10.

The scaling relations presented in this Letter are important for studying the RM unstable systems driven by strong shocks. It allows us to obtain the results for all strong shocks by conducting only one strong shock experiment or by performing one strong shock numerical simulation in that family. We have checked that this scaling relation also holds for RM unstable interfaces driven by strong shock in planar geometry. We believe that this relation should hold in spherical geometry as well. We further speculate that this scaling law also holds for multimode RM unstable systems driven by strong shocks.

We would like to thank Dr. I-Liang Chern for helpful discussions. This work was supported in part by the U.S. Department of Energy, Contract No. DE-FG02-90ER25084 and National Science Foundation, Contract No. NSF-DMS-9301200.

[1] G. Dimonte, C. E. Frerking, and M. Schneider, Phys. Plasmas **3**, 614–630 (1996).
[2] R. D. Richtmyer, Commun. Pure Appl. Math. **13**, 297–319 (1960).
[3] E. E. Meshkov, NASA Tech. Trans. **F-13**, 074 (1970).
[4] G. Fraley, Phys. Fluids **29**, 376–386 (1986).
[5] K. A. Meyer and P. J. Blewett, Phys. Fluids **15**, 753–759 (1972).
[6] Y. Yang, Q. Zhang, and D. H. Sharp, Phys. Fluids **6**, 1856–1873 (1994).
[7] R. Menikoff and C. Zemach, J. Comput. Phys. **51**, 28–64 (1983).
[8] J. Hecht, U. Alon, and D. Shvarts, Phys. Fluids **6**, 4019–4030 (1994).
[9] Q. Zhang and S. Sohn, Phys. Lett. A **212**, 149–155 (1996).
[10] K. O. Mikaelian, Phys. Rev. Lett. **71**, 2903–2906 (1993).
[11] S. Haan, Phys. Fluids B **3**, 2349–2355 (1991).
[12] R. Samtaney and N. J. Zabusky, Phys. Fluids A **5**, 1285–1287 (1993).
[13] E. Meshkov, in *Advances in Compressible Turbulent Mixing* (National Technical Information Service, U.S. Department of Commerce, Springfield, VA, 1992), pp. 473–503.
[14] R. Benjamin *et al.*, in *Proceedings of Third International Workshop on the Physics of Compressible Turbulent Mixing, Royaumont, France, 1991*, edited by D. Besnard (CEA DAM, Villeneuve St.-George, France, 1991), pp. 325–332.
[15] S. Zaytsev, A. Aleshin, E. Lazareva, S. Titov, E. Chebotareva, V. Rozanov, I. Lebo, and V. Demchenko, in *Proceedings of Third International Workshop on the Physics of Compressible Turbulent Mixing, Royaumont, France, 1991* (Ref. [14]), pp. 57–62.
[16] R. Benjamin, D. Besnard, and J. Hass, Los Alamos National Laboratory Report No. LA-UR 92-1185, 1992.
[17] J. W. Grove, R. Holmes, D. H. Sharp, Y. Yang, and Q. Zhang, Phys. Rev. Lett. **71**, 3473–3476 (1993).
[18] R. Holmes, J. Grove, and D. Sharp, J. Fluid Mech. **301**, 51–64 (1995).
[19] L. D. Cloutman and M. F. Wehner, Phys. Fluids A **4**, 1821–1830 (1992).
[20] T. Pham and D. Meiron, in *Proceedings of Third International Workshop on The Physics of Compressible Turbulent Mixing, Royaumont, France, 1991* (Ref. [14]), pp. 145–153.
[21] U. Alon, J. Hecht, D. Mukamel, and D. Shvarts, Phys. Rev. Lett. **72**, 2867–2870 (1994).
[22] D. L. Youngs, Lasers Part. Beams **12**, 725–750 (1994).
[23] I-L. Chern, J. Glimm, O. McBryan, B. Plohr, and S. Yaniv, J. Comput. Phys. **62**, 83–110 (1986).